



Optimization of biaxial tensile specimen shape from numerical investigations

Ibrahim Zidane, Cunsheng Zhang, Dominique Guines, Lionel Leotoing, Eric Ragneau

► To cite this version:

Ibrahim Zidane, Cunsheng Zhang, Dominique Guines, Lionel Leotoing, Eric Ragneau. Optimization of biaxial tensile specimen shape from numerical investigations. Numisheet 2008, Sep 2008, Interlaken, Switzerland. pp.1-6. hal-00941797

HAL Id: hal-00941797

<https://hal.science/hal-00941797>

Submitted on 4 Feb 2014

HAL is a multi-disciplinary open access archive for the deposit and dissemination of scientific research documents, whether they are published or not. The documents may come from teaching and research institutions in France or abroad, or from public or private research centers.

L'archive ouverte pluridisciplinaire **HAL**, est destinée au dépôt et à la diffusion de documents scientifiques de niveau recherche, publiés ou non, émanant des établissements d'enseignement et de recherche français ou étrangers, des laboratoires publics ou privés.

OPTIMISATION OF BIAXIAL TENSILE SPECIMEN SHAPE FROM NUMERICAL INVESTIGATIONS

I. Zidane^{*}, C. Zhang, D. Guines, L. Léotoing, E. Ragneau

Insa de rennes – LGCGM EA3913

ABSTRACT: In innovative industrial processes such as hydroforming or incremental forming, strain rates up to 500s^{-1} can be reached. As a result, experimental setups allowing to obtain large deformations from static to intermediate strain rate levels have to be developed to predict the formability limits of sheet metal materials. The proposed experimental device is a servo-hydraulic testing machine provided with four independent dynamic actuators allowing biaxial tensile tests on cruciform specimen. The main difficulty to define an appropriate cruciform specimen shape is to force the onset of necking in the central region. In this paper, different specimens used in previous studies are numerically investigated through FE simulations. A modified cruciform specimen shape is then proposed and the best set of geometrical dimensions is defined from a parametric study. Finally, the efficiency of the proposed specimen shape is validated by experiments. Numerical and experimental results, i.e., the strain level in the specimen and the onset of necking are compared and discussed to boundary conditions corresponding to an equi-biaxial tensile test.

KEYWORDS: Forming processes, dynamic tests, biaxial tensile, cruciform specimen, FE simulations.

1 INTRODUCTION

Simulation of sheet metal forming requires accurate constitutive models and prediction of formability limits of the material. Those material behaviors have to be characterized at strain, strain rate and temperature ranges corresponding to the process ones. The constitutive model describes into a single equation, the hardening behavior of the material as a function of strain, strain rate and temperature. The constants of these constitutive relationships are usually identified from force versus displacement curves through monoaxial tension tests. The determination of the forming limit diagram (FLD) is usually obtained from static conventional tests (Marciniak test [1], Nakazima test [2], bulge test [3], ...) by observing the onset of necking. In such tests, only linear loading paths can be realized. The paths are defined from the specimen geometry and many different specimens are required to cover the whole forming limit curve. Moreover, depending on the considered test, the friction effect between the specimen and the tool can influence the prediction of the material formability and it is still a difficulty to evaluate the coefficient friction value. Using an other technique, Andrews and Ellison [4] used thin-walled tubes solicited by traction-torsion loadings associated with an internal-external pressure to create bi-axial

stress/strain states. Although this technique appears to be efficient, it presents three major disadvantages [5]: - the stress-strain state is not exactly bi-axial because the radial stress caused by the pressure is not zero, - the level of temperature is often limited by the properties of fluid, - material anisotropy obtained by the tube extrusion is not compatible with the anisotropy of a sheet metal.

In order to overcome the drawbacks of the above mentioned tests, Pascole and Villiers [6], Hayhurst [7] and Kelly [8] use a plate cruciform specimen submitted to a static biaxial tensile in its plane. Depending on the device, two or four actuators are used and any ratio of biaxiality can be obtained by changing the proportion of the applied load or displacement [9].

Although cruciform specimens have been studied extensively, a general review on biaxial tensile tests and their applications proposed by Hannon and Tiernan [10] indicates that there is no standard geometry existing to this day. Moreover, in the whole of previous work published to date, the cruciform specimens were used within the framework of static characterizations of the behavior of the materials (anisotropy, work hardening, plasticity criteria) under biaxial solicitations. But in innovative industrial processes such as hydroforming or incremental forming, strain rates up to 500s^{-1} can be reached. As a result,

^{*} Corresponding author: 20 av. des Buttes de Coësmes, CS14315 – 35043 Rennes Cédex,
phone : 33 2 23 23 84 44, fax : 33 2 23 23 87 26, ibrahim.zidane@ens.insa-rennes.fr

Johnston and al [11] modified the specimen 1 and added a circular central zone with a smaller thickness (Figure 2).

[illegible]

Technical drawing of a mechanical part, labeled "Coupe B-B". The drawing shows a cross-section of a component with a central square hole and four vertical slots. Dimensions include a total width of 40, a central hole diameter of R10, and various radii (R4, R3, R7.0). A detail view shows a circular feature with a 1.5mm radius and a 1mm width.

The drawing shows a mechanical part with a cross-section and a top view. The cross-section, labeled "Coupe A-A", shows a part with a total width of 4, a central hole with a diameter of 2, and a thickness of 1. The top view shows a cross-shaped part with a central hole of diameter 30 and a radius of R10. The overall width of the part is 140, and the distance from the center to the outer edge is 30. The part has a fillet radius of R5 at the corners of the cross arms.

Replacing arm grooves, Yong and al [12] proposed the shape shown Figure 3. This form has been developed in order to determine the FLD under complex loading paths by numerical finite element simulations. The initial specimen dimensions defined by the authors lead to a very stiff

specimen: the arm width is 90mm and the central area diameter is 20mm. But to date, to our knowledge, no experimental results were published to validate this shape.

An other cruciform specimen shape (Figure 4) with reduced thickness in the central area and variable width arms has been proposed by Zhang and Sakane [13]. This specimen has been used to realize fatigue tests, i.e. to low strain levels.

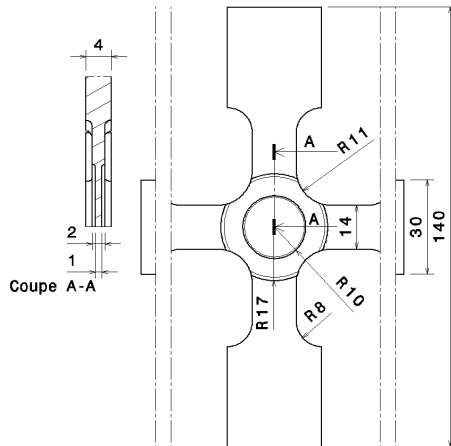


Figure 4: Dimensions of the specimen-4

2.1 FINITE ELEMENT ANALYSIS OF THE VARIOUS SPECIMEN SHAPES

Through FE simulations, the efficiency of the four various specimen shapes mentioned above is numerically investigated. For that, equi-biaxial tensile test is simulated by means of the FE software package ABAQUS. The selected material is an aluminium alloy (AA 2017) with an isotropic elastoplastic behavior. Considering the symmetry of the specimen geometries and the use of isotropic material, only one quarter of the specimen is analyzed. Tetrahedron elements are used to mesh the geometry and a refined particularly mesh is adopted in the sensitive areas where strain localizations can occur (central zone, intermediate section, fillet, grooves).

The various shapes suggested (figure 1 to 4) were dimensioned with the following rules:

- (i) the characteristic dimension of the central zone is fixed at a value ranging between 20 and 30mm. This dimension is mainly imposed by the acquisition capacities of the camera,
- (ii) other principal dimensions (width and thickness of the arms, thickness of the central area) are chosen according to either the maximum load capacities of the experimental setup or the maximum stiffness of the sample. The maximum value of this one is defined by the capacities of the experimental device. Consequently, the thickness of the central area and arms are respectively fixed to 1 and 4mm. For specimens 2 to 4, the thickness of the intermediate zone is 2mm.

2.2 RESULTS AND DISCUSSIONS

To ensure that necking always appears in the central zone, the design of the cruciform specimens must induce the greatest deformations in the central zone and no strain localizations in the other areas (grooves, fillet, ...). Both the equivalent plastic strain and the maximal principal strain in the specimen are observed. In the geometrical singularities (grooves for example), the observation of the equivalent plastic strain is not sufficient, since the major principal strain can reach high values leading to a localization of the deformation (then the rupture will appear in this point) although the equivalent strain is not very high. The figures 5 and 6 show the equivalent plastic strain (PEEQ) and the maximal principal strain fields for respectively the specimens 1 to 4. Only the interesting zone, i.e. the central zone is presented. All the results presented correspond to the moment when the maximum value of the equivalent plastic strain reaches 30% in a point of the specimen. In order to evaluate the influence of the shape details such as the grooves, the fillet of the arms, the evolution of the strain (equivalent plastic and maximal principal) is also plotted along a path (represented by a mixed line).

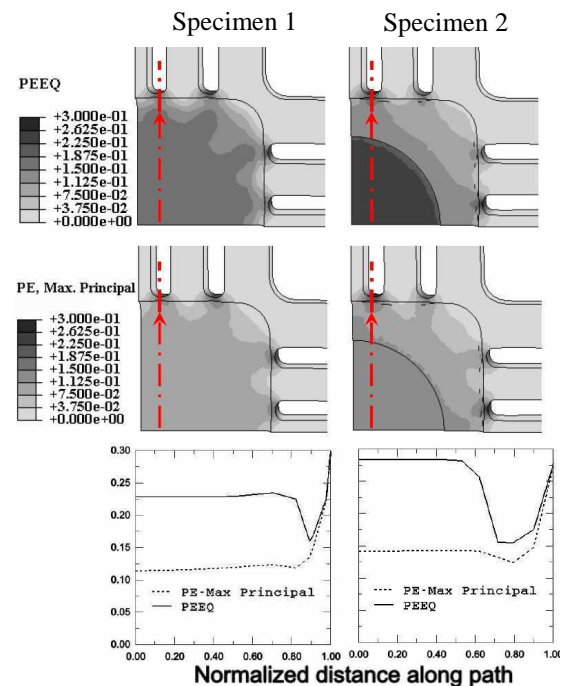


Figure 5: Equivalent plastic strain and maximal principal strain fields for specimens 1 and 2

According to figures 5 and 6, one can see that the strain concentration is more homogeneous in the central test section of the specimens with grooves (specimens 1 and 2). But, for the specimen 1, the maximum strain value (30%) is reached in the grooves. This phenomenon is less pronounced for specimen 2 where an intermediate zone has been added. The equivalent plastic strain is then slightly

higher in the central zone than in the grooves. But, the maximal principal strain is always much higher (27.5%) in those last ones than in the central area (15%).

For the specimen 3, the maximal principal strain is obtained in the fillet of the arms (25%) whereas in the central zone the level reached is approximately 15%.

For the specimen 4, the highest strain values (maximal principal strain or equivalent plastic strain) are located in the fillet of the arms whereas in the central area, the value of the maximum principal strain is the lowest one of those obtained on the 4 specimens (11%).

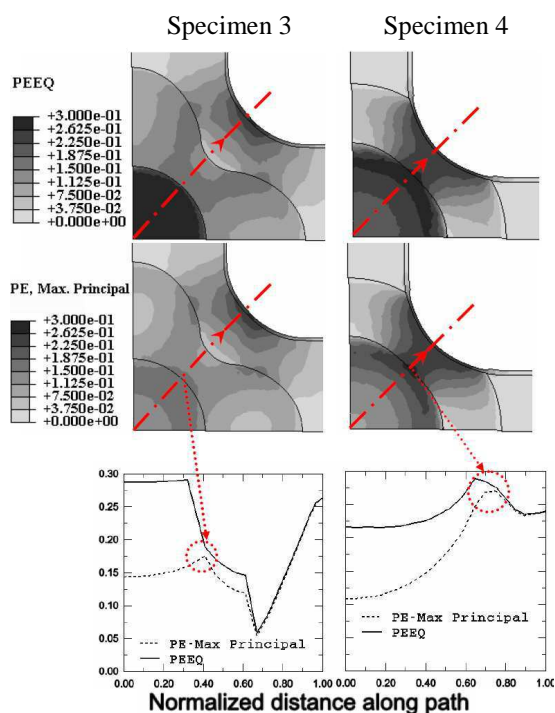


Figure 6: Equivalent plastic strain and maximal principal strain fields for specimens 3 and 4

Table 1: Stiffnesses of the tested specimens

Specimens	1	2	3	4
Stiffness (KN/mm)	42	45	62	38

The results of the FE simulations show that the specimen 2 and 3 seem to be the more efficient specimens since they lead to the maximum values of strain in the central zone among the 4 specimens tested. Specimen 3 is, for all the specimens tested, stiffest (Tab. 1). Moreover, to reduce the stress/strain concentrations in the fillets of the arms, it would be advisable to increase the width of the arms but that would result in increasing the stiffness of the specimen. Finally, the shape of specimen proposed figure 2 seems most effective and most promising. The positioning of the grooves on the arms make it possible to limit the stiffness of the specimen. An optimization can be

performed, FE simulations show notably that the distance between the ends of the grooves and the edge of the square central zone, had a great influence on the level of deformation in the grooves or fillets of the arms.

Thereafter, on the basis of the shape of the sample 2, a modified form is proposed and optimized in order to reduce the strain localization in the grooves.

3 OPTIMIZED CRUCIFORM SPECIMEN SHAPE

A modification of specimen 2 is proposed by replacing the fillet between the central circular zone and the intermediate square zone by a chamfer with an outer diameter of 25mm (Figure 7). The aim of the chamfer is to improve the strain homogeneity and localization in the central test section.

According to the preliminary study, four important geometric parameters (Figure 7) have been identified: - the length L between the ends of the grooves and the edge of the square central zone, - the fillet of arms R_c , - the thickness of the central test section T , - the diameter of the central test section D_i .

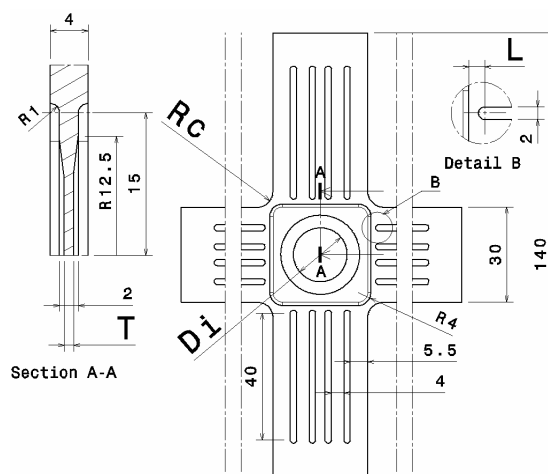


Figure 7: Geometry of the optimized specimen shape

A parametric study was carried out and the best set of parameters obtained is the following:

$L = 4.5\text{mm}$; $R_c = 8\text{mm}$; $D_i = 10\text{mm}$; $T = 0.75\text{mm}$

The figures 8 and 9 show respectively the strain fields and the evolution of strain in function of the tensile displacement for the optimized shape given above. As one can see it in figure 8, the strain fields are homogeneous in the central zone. Moreover, the equivalent plastic strain and the maximal principal strain are always greater in the central zone than anywhere in the specimen (figure 9). Numerically, the necking well appears in the central area.

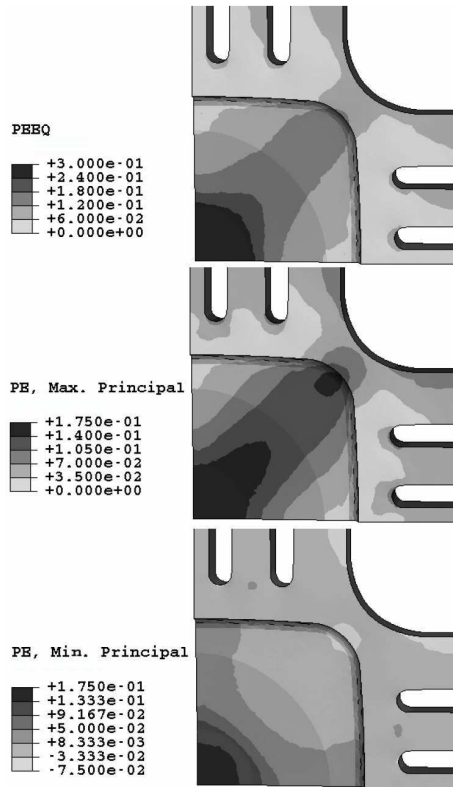


Figure 8: Equivalent plastic strain and principal strain fields

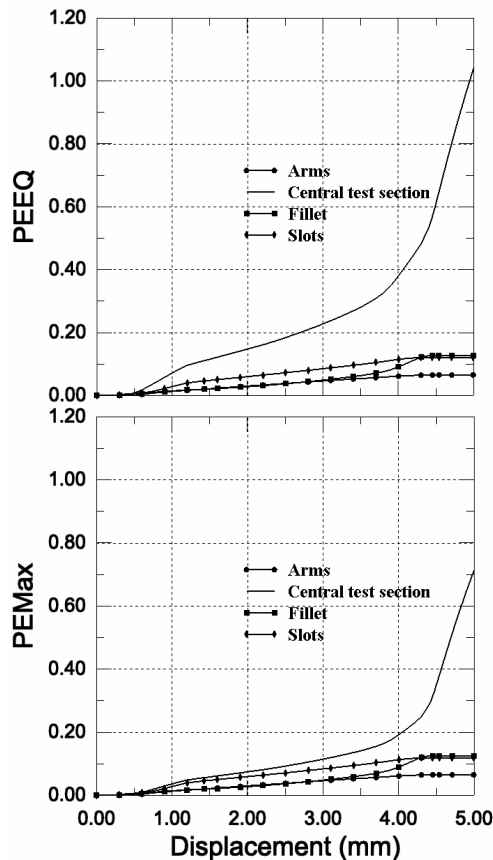


Figure 9: Evolution of equivalent plastic strain and maximal principal strain in function of the actuator displacement

4 COMPARISON BETWEEN EXPERIMENTS AND FE RESULTS

The experimental device is a servo-hydraulic testing machine provided with four independent dynamic actuators. The central area of the cruciform specimen is filmed with a camera. In order to validate the defined shape of the specimen, a static equi-biaxial test has been performed. A velocity of 1mm.s^{-1} is applied on each actuator. The sample is machined in a rolled aluminium alloy sheet (AA 2017).

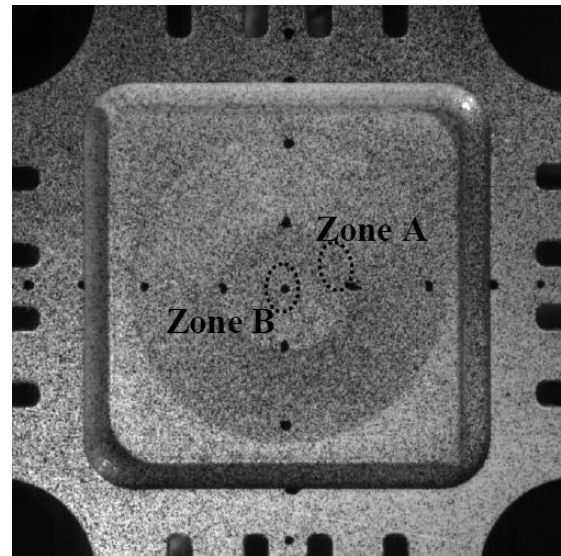


Figure 10: Central zone of the specimen tested

In the figure 10, one can see an image of the specimen before the test. The strain fields are determined by means of a digital image correlation technique. The results of the image post-processing presented figure 11 show that a biaxial state of deformation is well obtained in the center of the specimen (zone B).

For the studied material, the results allow to identify the onset of necking in the zone A (figure 11) with a maximal principal strain of 16% and a minimal principal strain of 6%.

The comparison of the experimental results and the numerical results reveals however differences in the strain versus displacement curves: the slopes of the experimental curves are different from those obtained numerically (either for the equivalent plastic deformation or for the maximal principal strain), the strain levels are also different. This can be explained by the material behavior considered in the FE simulations. Indeed, numerical simulations have shown a great influence of the hardening law on the strain evolutions. The simplistic isotropic hardening law introduced in the FE simulations has been established from an uniaxial tensile test in the roll direction.

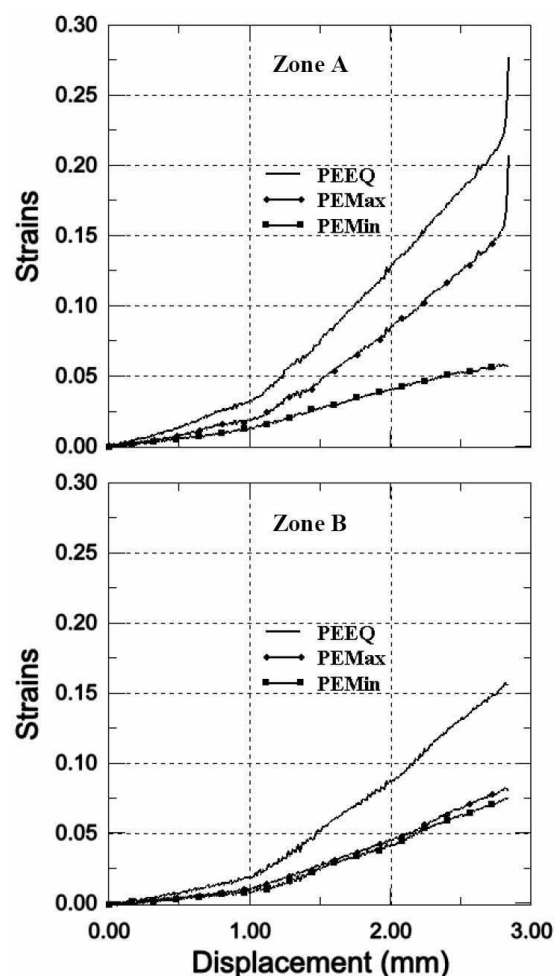


Figure 11: Experimental results

5 CONCLUSIONS

Through numerical FE simulations, various cruciform specimen shapes have been investigated. A parametric study leads to the definition of an efficient shape for which the strain localization appears in the central zone. The numerical approach has been validated by experiment. The onset of necking has been well observed and measured in the zone of interest. From this cruciform specimen shape, different strain paths can be applied to determine the whole FLD independently of any friction phenomena. A great influence of the constitutive law on the strain level has been observed.

6 REFERENCES

- [1] Marciniak Z. Kuczynski K. Pokora T.: *Influence of the plastic properties of a material on the forming limit diagram for sheet metal in tension*. Int. J. Mech. Sci, 15: 789–805, 1973.
- [2] Nakazima K. Kikuma T. Hasuka K.: *Study on the formability of steel sheets*. Yamata Technical Report. 264: 141-154, 1968.

- [3] Duddedar T. D. Koch F.B. Doeries E.M.: *Measurement of shapes of foil bulge test samples*. EXP. Mech., 17: 133-140, 1977.
- [4] Andrews J M H. Ellison E G.: *A testing rig for cyclic at high biaxial strains*. Journal of Strain Analysis, 8 (3): 168-175, 1975.
- [5] Demmerle S. Boehler J.: *Optimal design of biaxial tensile cruciform specimens*. Journal of the mechanics and physics, 41(1): 143-181, 1993.
- [6] Pascole K. J. De Villiers J. W. R.: *Low cycle fatigue of steels under biaxial straining*. Journal of Strain Analysis, 2 (2): 117-126, 1967.
- [7] Hayhurst D. R.: *A biaxial-tension creep-rupture testing machine*. Journal of Strain Analysis, 8 (2): 119- 123, 1973.
- [8] Kelly D. A.: *Problems in creep testing under biaxial stress systems*. Journal of Strain Analysis, 11 (1): 1- 6, 1976.
- [9] Xiang-Dong W., Min W. Xian-Bin Z.: *Biaxial tensile testing of cruciform specimen under complex loading*. Journal of Materials Processing Technology, 168: 181–183, 2005.
- [10] Hannon A. Tiernan P. *A review of planar biaxial tensile test systems for sheet metal*. Journal of Materials Processing Technology, 198: 1-8, 2008.
- [11] Johnston W. M. Pollock W. D. Dawicke D. S.: *Biaxial Testing of 2195 Aluminum Alloy Using Cruciform Specimens*. Analytical Services & Materials, Inc. Hampton, Virginia, NASA/CR211942, 2002.
- [12] Yong Y. Min W. Xiang-Dong W. Xian-bin Z.: *Design of a cruciform biaxial tensile specimen for limit strain analysis by FEM*. Journal of Materials Processing Technology, 123: 64-70, 2002.
- [13] Zhang S. et Sakane M.: *Multiaxial creep-fatigue life prediction for cruciform specimen*. International Journal of Fatigue, 1: 1-9, 2007.
- [14] Ferron G. Makinde A.: *Design and development of a biaxial strength testing device*. Journal of Testing and Evaluation, 16: 253–256, 1988.